NASA/TM-20205011477 AIAA–2020–3571

Thermal Management System Design for Electrified Aircraft Propulsion Concepts

Jeffryes W. Chapman, Hashmatullah Hasseeb, and Sydney Schnulo
Glenn Research Center, Cleveland, Ohio

March 2021

NASA STI Program . . . in Profile

Since its founding, NASA has been dedicated to the advancement of aeronautics and space science. The NASA Scientific and Technical Information (STI) Program plays a key part in helping NASA maintain this important role.

The NASA STI Program operates under the auspices of the Agency Chief Information Officer. It collects, organizes, provides for archiving, and disseminates NASA's STI. The NASA STI Program provides access to the NASA Technical Report Server—Registered (NTRS Reg) and NASA Technical Report Server—Public (NTRS) thus providing one of the largest collections of aeronautical and space science STI in the world. Results are published in both non-NASA channels and by NASA in the NASA STI Report Series, which includes the following report types:

- TECHNICAL PUBLICATION. Reports of completed research or a major significant phase of research that present the results of NASA programs and include extensive data or theoretical analysis. Includes compilations of significant scientific and technical data and information deemed to be of continuing reference value. NASA counter-part of peer-reviewed formal professional papers, but has less stringent limitations on manuscript length and extent of graphic presentations.

- TECHNICAL MEMORANDUM. Scientific and technical findings that are preliminary or of specialized interest, e.g., "quick-release" reports, working papers, and bibliographies that contain minimal annotation. Does not contain extensive analysis.

- CONTRACTOR REPORT. Scientific and technical findings by NASA-sponsored contractors and grantees.

- CONFERENCE PUBLICATION. Collected papers from scientific and technical conferences, symposia, seminars, or other meetings sponsored or co-sponsored by NASA.

- SPECIAL PUBLICATION. Scientific, technical, or historical information from NASA programs, projects, and missions, often concerned with subjects having substantial public interest.

- TECHNICAL TRANSLATION. English-language translations of foreign scientific and technical material pertinent to NASA's mission.

For more information about the NASA STI program, see the following:

- Access the NASA STI program home page at http://www.sti.nasa.gov

- E-mail your question to help@sti.nasa.gov

- Fax your question to the NASA STI Information Desk at 757-864-6500

- Telephone the NASA STI Information Desk at 757-864-9658

- Write to:
  NASA STI Program
  Mail Stop 148
  NASA Langley Research Center
  Hampton, VA 23681-2199

NASA/TM-20205011477 AIAA–2020–3571

Thermal Management System Design for Electrified Aircraft Propulsion Concepts

Jeffryes W. Chapman, Hashmatullah Hasseeb, and Sydney Schnulo
Glenn Research Center, Cleveland, Ohio

Prepared for the
AIAA Propulsion and Energy 2020 Forum
sponsored by the American Institute of Aeronautics and Astronautics
Virtual Event, August 24–28, 2020

National Aeronautics and
Space Administration

Glenn Research Center
Cleveland, Ohio 44135

March 2021

Acknowledgments

The authors would like to thank NASA's Convergent Aeronautics Solutions (CAS) and Revolutionary Vertical Lift Technology (RVLT) projects for the funding of this work. The authors would also like to thank Patrick Hanlon of NASA Glenn Research Center (GRC) for his help in defining the electric system architectures, as well as Jason Kirk, Kevin Antcliff, and Zachery Fredrick of NASA Langley Research Center (LaRC) for providing vehicle objective functions. We would also like to thank Charles Lents of United Technologies Research Center for his expertise in thermal management systems.

Level of Review: This material has been technically reviewed by technical management.

Available from

NASA STI Program
Mail Stop 148
NASA Langley Research Center
Hampton, VA 23681-2199

National Technical Information Service
5285 Port Royal Road
Springfield, VA 22161
703-605-6000

This report is available in electronic form at http://www.sti.nasa.gov/ and http://ntrs.nasa.gov/

Thermal Management System Design for Electrified Aircraft Propulsion Concepts

Jeffryes W. Chapman, Hashmatullah Hasseeb, and Sydney Schnulo
National Aeronautics and Space Administration
Glenn Research Center
Cleveland, Ohio 44135

Abstract

This paper describes the development of thermal management systems (TMS) for three electrified aircraft propulsion (EAP) vehicle concepts released by NASA that span the UAM, regional, and single-aisle markets. For each EAP concept, a conventional TMS is designed for two electric component technology levels: state of the art and advanced. The goals for the paper are to compare the TMS designs for the above EAP concepts, to study how changes in requirements affect the TMS subcomponents, and to develop generalized TMS sizing relations. Each conventional TMS concept utilizes a liquid-based cooling methodology and is designed to cool the EAP electrical components only. The design parameters considered in this study include TMS architecture variation due to differing vehicle cooling requirements, electrical component efficiencies, vehicle total fuel burn or energy consumption, and electrical component operating temperatures. Results show that cooling components with low temperature limits increases TMS weight and demonstrate that efficiency gains of the specific technologies can net a lower weight TMS system despite more stringent temperature limits.

Nomenclature

BLI	Boundary Layer Ingestion
CTOL	Conventional TakeOff and Landing
EAP	Electrified Aircraft Propulsion
FOC	Fuel Oil Cooler
GBX	Gearbox
HEMM	High Efficiency Megawatt Motor
MN	Mach Number
pax	Passenger
PEGASUS	Parallel Electric-Gas Architecture with Synergistic Utilization Scheme
PGW30	Propylene Glycol Water 30%
PSF-5	Pure Silicone Fluid with a viscosity of 5cSt
RTO	Rolling TakeOff
RVLT	Revolutionary Vertical Lift Technology project
SNOPT	Sparse Nonlinear OPTimizer
SOA	State Of the Art
STARC-ABL	Single-aisle Turboelectric AiRCraft with an Aft Boundary-Layer propulsor
TMS	Thermal Management System
TOGW	TakeOff Gross Weight
UAM	Urban Air Mobility
VTOL	Vertical TakeOff and Landing

I. Introduction

In the last decade, NASA has continued investing in Electrified Aircraft Propulsion (EAP) research. This research is driven by potential improvements in fuel efficiency, emissions, and noise levels. [1] EAP may be an enabling technology for Urban Air Mobility (UAM), which includes last-mile delivery, air metro, air ambulance, and air taxi concepts. [2] The UAM opportunity offers a market changing concept estimated to be a billion dollar industry by 2030. [3] In order to realize the gains EAP vehicles introduce, additional electrical systems, such as higher-powered generators, power conditioning electronics, and motors, must be introduced to the aircraft. In a typical jet engine, waste heat is rejected through the exhaust of the engine; however, in EAP vehicles, the additional electric components generate a low grade or low temperature, heat that cannot be rejected in this way.

One method of cooling these components is with a conventional thermal management system (TMS) that utilizes liquid based heat exchangers. Here, waste heat is transferred via a coolant to a heat exchanger that rejects the heat to the atmosphere. This paper will explore the development of conventional TMS designs for three vehicles, the Single-Aisle Turboelectric Aircraft with an Aft Boundary Layer propulsor (STARC-ABL), [4] a turbo-electric tiltwing Vertical Takeoff and Landing (VTOL) vehicle developed by the Revolutionary Vertical Lift Technology (RVLT) project [5], and the Parallel Electric-Gas Architecture with Synergistic Utilization Scheme (PEGASUS) [6]. These architectures will be evaluated at two different electrical system technology levels, a baseline state of the art (SOA) system and an advanced level, which takes into account research goals of efficiency and specific power. These concept designs will be compared to show how system architecture, component temperature constraints, and component efficiencies affect the TMS design.

The three vehicles studied in this paper, as shown in Figure 1 and defined in Table 1, offer very different EAP platforms. The STARC-ABL is designed for a single-aisle 154 passenger (pax) commercial transport mission, utilizes a classic tube-and-wing concept, and supports conventional takeoff and landing (CTOL). The propulsion system consists of two wing-mounted turbofans that provide thrust as well as power to an electrically driven tail mounted fan. The EAP portions of STARC-ABL are turbo-electric with no plans for a substantial battery. The 15 pax RVLT tiltwing vehicle is designed for a UAM mission with 8 legs of 50 nm each with vertical takeoff and landing at the start and end of each leg respectively. This concept is a true turbo-electric vehicle with a single turboshaft generating power for four wing-mounted propellers. The onboard battery is used for emergency backup only, therefore it will not be considered in this study. The final vehicle, PEGASUS, is a 48 pax aircraft designed for regional commuting or short haul and consists of two wing tip, two wing inboard, and one, rear tail propellers. At the start of cruise the inboard-mounted propellers fold back and turn off so that the wing tip mounted propellers provide the majority of thrust. This paper considers the 200 nm all-electric mission. To accomplish this mission, the PEGASUS contains a large 13,000 lbm battery (~24% of takeoff gross weight (TOGW)). [6,7]

Table 1. Vehicle concept summary.

Concept	Type	Range (nm)	Cruise altitude (ft)	Cruise speed (MN)	pax	Number of Propulsors			Engines	Battery	TOGW (lbm)
						Total	Electrically Driven	Engine Driven			
STARC-ABL	CTOL	3500	35,000	0.7	154	3	1	2	2	No	133,370
Tiltwing	VTOL	400	10,000	0.3	15	4	4	0	1	Yes	13,866
PEGASUS (all electric)	CTOL	200	20,000	0.48	48	5	5	0	2	Yes	53,041

Figure 1. Considered aircraft concepts: tiltwing (top), STARC-ABL (bottom left), and PEGASUS (bottom right), not to scale.

Since this paper is generally about TMS design, only electrical component efficiency and temperature limits for the two electrical system technology levels are considered. These efficiencies and limits are tabulated in Table 2. Baseline motor and power converter (AC-DC, rectifier, or DC-AC, inverter) efficiencies and temperature limits were gathered from literature ([4], [8], [9]) and assumed based on engineering judgement. The baseline configuration represents state of the art technology and relies on a DC electrical bus. The advanced EAP power system is based on three major technological advancements: the High Efficiency Megawatt Motor (HEMM), a low weight and efficient electrical transmission scheme, and high efficiency converters. [10] The HEMM utilizes a superconducting rotor coil and cryogenic cooling to increase motor efficiency, [11] which comes at the price of a reduced operating temperature (60 C) as compared to baseline motors (106 C). The proposed electrical transmission technology utilizes an AC bus over the more common DC bus. This reduces transmission wiring weight and the need for power conversion. [12] High efficiency DC-link converters that utilize interleaving has been estimated to increase converter efficiency to 99.5%. [13] It should be noted that, an AC-to-AC conversion that utilizes DC-link converters results in an overall efficiency of 99%. In this study, baseline and advanced battery technology are both assumed to be Lithium ion with temperature limits defined by current specifications. [14] Analysis for the single aisle concept within this paper is part of a larger study that considers the entire system in more detail. For more details on the electrical system or other vehicle components this larger study can be referenced. [15]

Table 2. Electrical component efficiencies and temperature requirements.

		Motor/ Generator	Electric Converter	Battery*
Efficiencies	Baseline Current	96%	98%	92%
	Advanced	98.5%	99.5%	92%
Baseline Technology Temperature Limits	Coolant In (C)	106	54	35[54]
	Coolant Out (C)	150	60	45[60]
Advanced Technology Temperature Limits	Coolant In (C)	60	54	35[54]
	Coolant Out (C)	68	60	45[60]

*defined temperature limits are a constant power number and the number in brackets is a maximum temperature limit that may be used for shorter durations(up to 10 min duration). As defined, the short duration number can be used for takeoff and the constant power number can be used for cruise.

Simulation techniques and design methodology used in this study are a continuation of work done in Reference [9], where a full definition of the theory is put forth. As a summary, the framework is 0-D and relies on Kays and London [16] techniques to estimate heat exchanger performance, pressure drop, and effectiveness. Components such

as coolant lines and pumps are treated as ideal and compressible flow is analyzed with isentropic processes or with ideal pressure drops. The goal of this modeling framework is to determine TMS metrics (weight, power used, and drag) that can then be applied to the overall aircraft conceptual analysis. The TMS design considers a compact plate-fin type heat exchanger that is optimized utilizing sizes, coolant flows, and temperatures as the design variables, which are constrained by sets of component hardware constraints. Architectures and cooling fluids for each TMS system are selected based on engineering requirements and objective functions that were defined by the vehicle mission profile. Each simulation is written in Python using the OpenMDAO framework [17] and optimizations are executed using the Sparse Nonlinear OPTimizer (SNOPT). [18]

Subsequent sections of this paper detail the sensitivity study and vehicle specific TMS designs. A single loop design process and sensitivity study will be detailed in Section II. In Section III, each vehicle TMS architecture and requirements will be detailed at both technology levels. Final results and comparisons will be included in Section IV. And finally, the summary and conclusions will be given in Section V.

II. Overview of TMS Design and Simulation

The major contributors to a TMS design are component temperature limits, the amount of heat rejected, and the environmental conditions surrounding the system. This section contains sensitivity studies of these design factors considering a simple heat exchanger network. This network consists of a coolant loop with a heat load and a heat exchanger that rejects energy to the air. As shown in Figure 2, the coolant is pumped while air is fed through the heat exchanger via a puller fan or inlet ram air. The choice to use a puller fan or ram air is dictated by the pressure drop requirement of the air side of the heat exchanger. Essentially in low speed applications, where ram air does not generate enough pressure to overcome the heat exchanger pressure drop, a puller fan is required. This choice will be reflected in the drag and power used by the system, where a ram air fed system will generate drag and use less power and a puller fan system will generate positive thrust and require more power. The objective used for the system optimizations is stated as a function of weight (kg), power used (kW), and drag (lbf) and is shown in equation 1.

$$Objective = 3.5e2 * Weight + 6.5 * PowerUsed + 2.0e2 * Drag \quad (1)$$

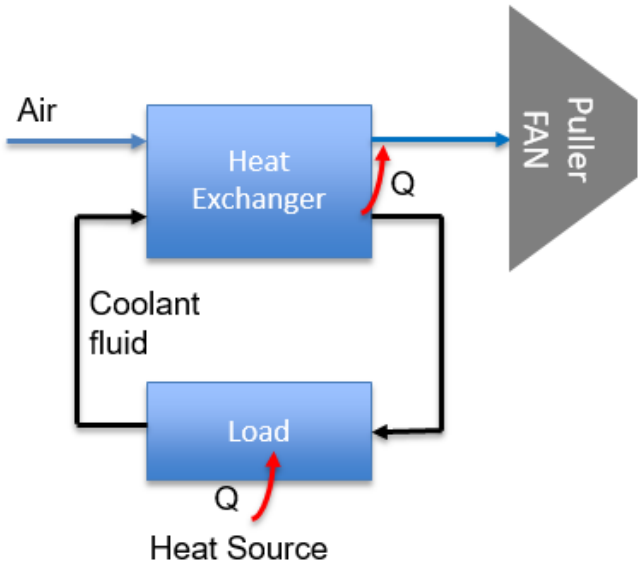

Figure 2. Simple TMS system.

In the following two sub-sections, TMS design sensitivities are explored. In section A, a sensitivity study of how TMS designs change with heat load and temperature limits is demonstrated. Then in section B, different altitudes and Mach numbers are examined to determine how TMS design point choice can affect a final TMS design.

A. Temperature Limit and Heat Load Sensitivity

The first study in this paper examines the effects of heat load rejection and component temperature limits on the TMS design. In this study, for a hot 40 C day, the rejected heat load was varied from 5 kW to 300 kW while the component inlet temperature was varied from 60 to 110 C. For all cases run, coolant and air mass flow was limited to 40 kg/s and heat exchanger size was limited to 125 m^3. The sensitivity of the design to these parameters is captured in Figure 3, where their effect on total TMS weight, net thrust produced, required TMS power and required air mass flow rate is examined. It should be noted that the power required to run the TMS consists of two major contributors: the power required to pump the coolant and the power required to operate the puller fan.

For cases where the inlet temperature limit is greater than 60 C, the analysis shows there is generally a linear trend with increasing power rejection. Increases in heat exchanger coolant inlet temperature (corresponding to load temperature limit) decrease the metrics in a non-linear fashion. In the 60 C case, the response is linear until 100 kW of rejected heat is reached. At this point the maximum air flow limit is hit, which causes thrust to level off, weight (heat exchanger size, which reduces heat exchanger pressure drop) to increase non-linearly, causing power required to drop. At each test temperature there is also a non-linear response at low heat load rejection levels (under 20 kW rejected power), where the metrics begin to shrink at a more rapid rate. Note, in these traces net thrust is generated due to the use of puller fans.

An important observation to make is how beneficial higher temperature limits are to the overall TMS design. As will be highlighted in an example, the benefits these laxer limits provide are similar to those garnered in using more efficient electrical components. Consider a system with a 300 kW load and a 70 ℃ temperature limit. Based on Figure 3, if the temperature limit were to increase to 80 C then the resulting TMS redesign has a 23% reduction in weight, required TMS power, and net thrust for the TMS. These benefits can alternatively be obtained if the electrical component loss were instead reduced by a third (i.e. to 200 kW). This further highlights the need for EAP vehicles and their components to widen their operating temperature limits and also increase component efficiencies in order to generate feasible TMS designs.

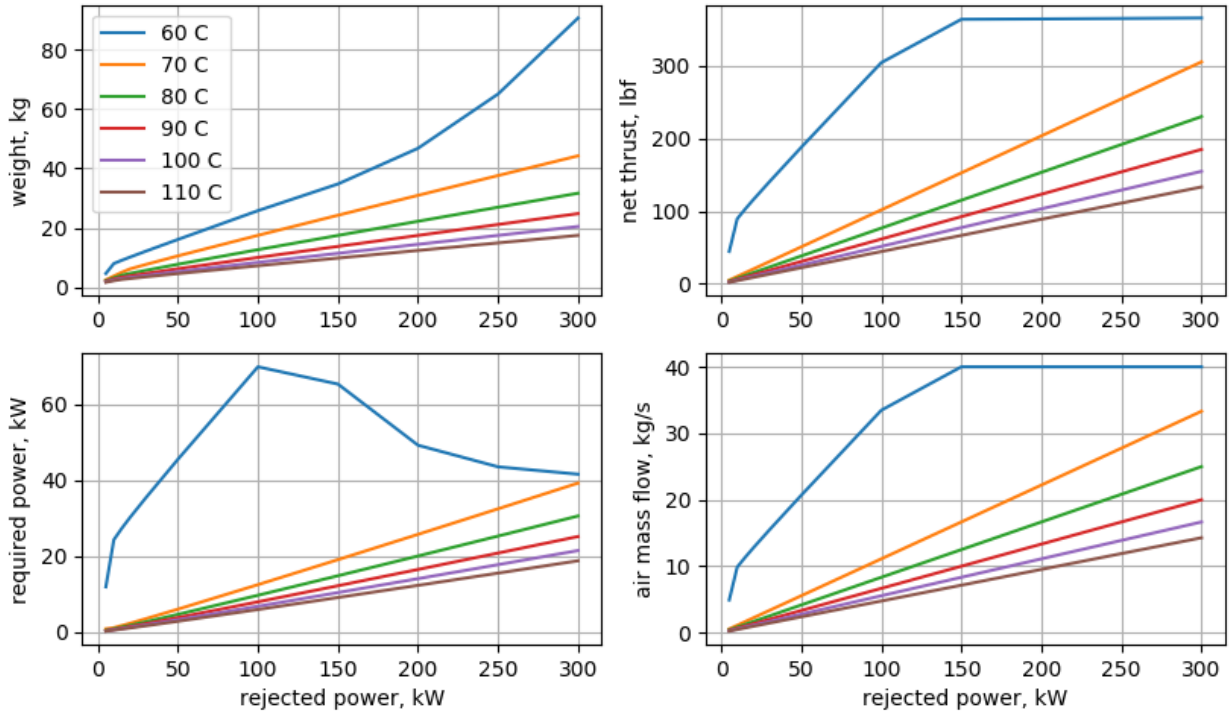

Figure 3. TMS design sensitivity to rejected power and temperature limits.

B. Altitude and Mach Number Sensitivity

The second study in this paper considers the effect of altitude and Mach number (MN) on the TMS design, given a constant 30 kW heat load. The study also considers three objective configurations: default from equation 1, reduced power required weighting, and reduced thrust weighting. A notional mission has been developed. The mission points are categorized into three phases and are summarized in Table 3. Environmental conditions for the mission correspond to a hot day (international standard atmosphere + 25 C) and limits align with cooling electrical components. Using points along the profile, different TMS designs result, as shown in Figure 4.

Table 3. Notional aircraft mission points.

Phase	Mission Point	Description
I	0-11	increase in speed from 0 to 0.2 MN at an altitude of 0 ft
II	11-20	climb in altitude from 0 to 20,000 ft at 0.2 MN
III	20-40	increase in speed from 0.2 to 0.5 MN at 20,000 ft

For the default objective in phase 1, the required power starts from a maximum value and drops significantly as MN increases. This large drop in required power coincides with an increase in TMS weight and a move from positive net thrust to drag. These trends are guided by the requirement for a puller fan, where designs with puller fans generate thrust as mass flow is forced through the heat exchanger and designs without puller fans generate drag as the vehicle must push mass flow through the heat exchanger. Since a puller fan is required at zero MN (there is no air flow), the optimization drives the heat exchanger smaller with a larger pressure drop and higher heat exchanger mass flow. As MN is increased, the power required to raise the exit air pressure with a puller fan increases, which causes the optimized design to reduce the size of the puller fan and increase the size of the heat exchanger. This simultaneously increases weight, to reduce the pressure drop across the heat exchanger. Once the puller fans are completely removed (roughly 0.15 MN), the weight increases and thrust decreases (more drag, no thrust generated by the puller fans), due to an increase in inlet temperature and inlet speed.

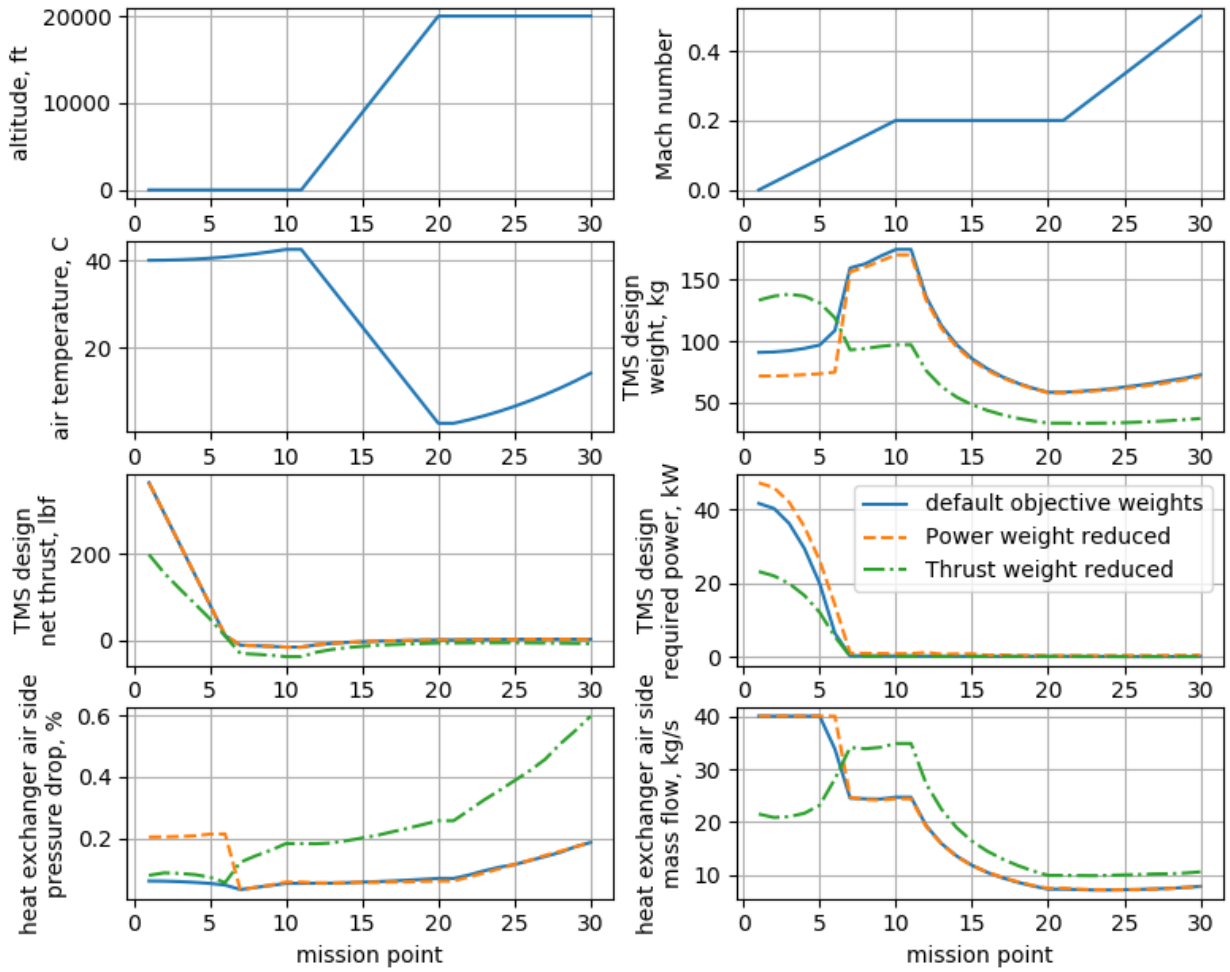

Figure 4. TMS designed at points along a notional aircraft mission.

During phase 2, the heat exchanger size decreases due to the lower temperatures at higher altitude. This causes TMS weight to be reduced and net thrust to rise (less drag) as less flow is required to maintain the heat rejection. In phase 3 vehicle speed increases, which causes an increase in temperature due to the compressibility effects. These changes result in only a marginal increase in weight and drag because, the updated design can make use of the increase in total pressure to increase the air side pressure drop, making a more effective heat exchanger design.

Adjusting the objectives used for the study causes some shift in the design. First, the power weighting for the objective is reduced by a factor of 10. With this adjustment, the phase 1 weight is consequently reduced while the required TMS power is increased. The resulting thrust remains nearly unchanged because the required air mass flow does not shift appreciably between the objectives. The phase 2 and 3 responses remain nearly unchanged with the default response due to the puller fans being removed and power levels being low.

If instead, the thrust weight in the objective is reduced by a factor of 10, then significant changes are observed. In phase 1, for example, the TMS weight is increased while the required power and thrust are reduced. This new balance coincides directly with a reduction in thrust weighting (remember that an increase in net thrust will decrease the objective). Once the puller fans are removed (roughly 0.15 MN) an increase in drag along with higher mass flows and pressure drop is observed in the design. This translates to a design using smaller heat exchangers with a larger drag penalty.

In choosing a design point, the thermal mass of each EAP component must be taken into account. In components with low thermal mass, the most conservative altitude and MN combination should be chosen because the component will heat up in a short amount of time. However, in larger components with higher thermal masses, such as the battery, a delay in full cooling along with potentially pre-mission cooling can be considered. [19]

If 20,000 ft can be reached before reaching a temperature limit (as Ref [19] suggests) then the sizing metrics within Figure 4 at 20,000 ft and 0.5 MN can be utilized resulting in a TMS weight savings of 60%. It should be noted that this analysis can be used to get a rough idea of the mission point sizing gains, but a fully transient simulation that takes into account thermal momentum should be used to determine a final design.

III. System Architectures and Designs

In this section, the three vehicle concepts are analyzed separately and the TMS architectures for each (baseline and advanced concept) are discussed in detail. Generally, the baseline TMS considers the electric components required to generate, transmit (using a DC bus), and utilize power. Advanced configurations use an AC bus and low loss components to minimize heat load. In some of the designs the electrical TMS will make use of the existing engine cooling loop. This is done to eliminate duplication of hardware and can only be done when location and temperature requirements are appropriate. In all cases that unitize this loop, the engine heat load is labeled as a gearbox, and assumed to be 2% of the generated engine shaft power. To make sure this is fairly accounted for, a corrected baseline is developed. The corrected baseline is generated by calculating an engine only TMS and then subtracting the system metrics from the baseline. This effectively removes the engine TMS contribution in order to demonstrate only the increase in TMS size due to the additional loads. This, as a result, allows the system to be compared directly with an electrical system TMS that is completely independent of the engine. For each system, engine oil, engine fuel, propylene glycol 30% (PGW30), and pure silicone fluid (PSF-5) are considered for the coolants, with operational limits shown in Table 4. Since engine oil is used for engine cooling and has a high operational temperature range, it will be limited to cool the baseline motors in this study. The PGW30 coolant was considered for electronics with low temperature requirements due to its high specific heat. The PSF-5 coolant is considered only because it is required for the HEMM motor, which requires a dielectric fluid for the direct cooling of its windings. Using fuel as a coolant in circulating cooling loops is typically not considered in civilian aircraft. However, using fuel as a coolant to increase engine efficiency by heating fuel prior to burning is a known boon to long range transports. To account for these trends, a fuel heating system was added to the STARC-ABL, due to its inclusion of an engine component and its long range mission. The electrical system and TMS designs for each system are included in the following subsections: (A) STARC-ABL, (B) RVLT tiltwing, and (C) PEGASUS.

Table 4. Coolant characteristics and limits.

Coolant Type	Maximum Operational Temperature (C)	Minimum Operational Temperature (C)	Specific Heat at maximum operating temperature (J/kg/C)	Application
engine oil	150	76	2444	engine
PGW30	106	35	4222	low temperature applications
PSF-5	135	35	1633	HEMM
Jet fuel	135	35	2388	engine

C. STARC-ABL

The baseline STARC-ABL electrical system architecture consists of two generators powering a DC bus, which operate a single motor powering a tail mounted fan. Power conversion for the baseline electrical architecture occurs after each generator (AC to DC) and before the motor (DC to AC). In contrast, the advanced electrical system architecture eliminates the power converter after the generator and utilizes two separate AC busses that run two distinct motors, as shown in Figure 5.

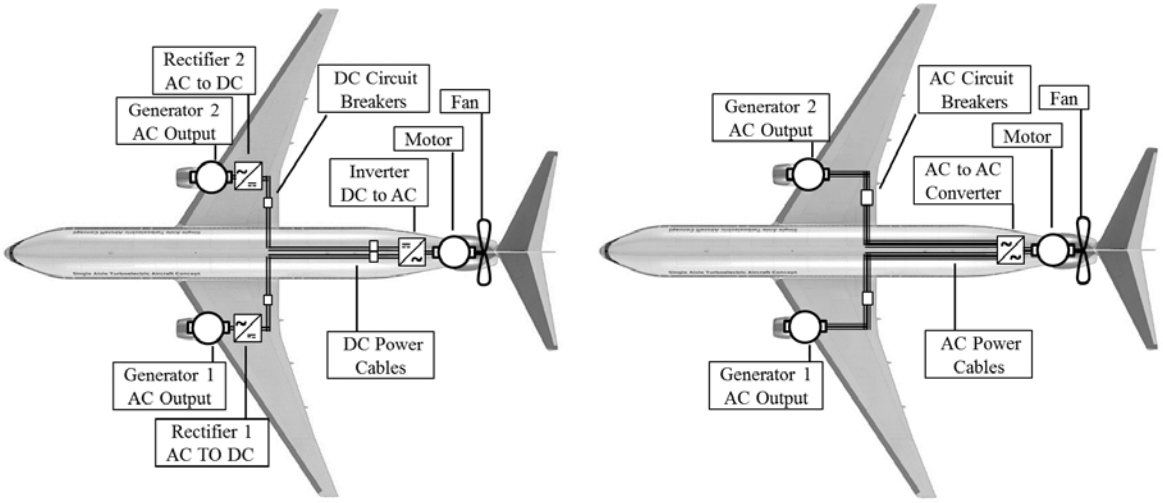

Figure 5. STARC-ABL EAP architecture for baseline (left) and advanced concepts (right).

The baseline TMS design for the STARC-ABL was divided into an engine oil loop, a rectifier loop and the tail mounted boundary-layer ingesting (BLI) fan loop, as shown in Figure 6. The baseline generator was added to the engine oil cooling loop, which uses engine bypass air to reject the heat to the environment, and utilizes a fuel-to-oil cooler (FOC). The generator's rectifier and controls require lower temperature cooling, so a second cooling loop utilizing PGW30 was added. A PGW30 coolant loop was also added to cool the motor and inverter of the BLI fan. A design point of rolling takeoff (RTO) was considered for this study with heat loads are shown in Table 5. It should be noted that fan air was only considered for cooling the engine oil loop. This is because air from the engine fan and BLI fan was found to be too high to provide adequate temperature margin for cooling electronics or the HEMM.

The advanced TMS heat loads and design architecture are shown in Table 5 and Figure 7, respectively. The total system loads for the baseline system are roughly 3 times higher than that of the advanced system loss if the gearbox is excluded. The advanced TMS is also simpler with the removal of the oil cooling loop and the replacement of the rectifier load with the generator load on the air cooling loop for the engine.

Table 5. STARC-ABL heat losses at RTO.

Baseline				Advanced			
Component	**Qty**	**Loss (kW)**	**Total loss (kW)**	**Component**	**Qty**	**Loss (kW)**	**Total loss (kW)**
Gearbox	2	116	232	-	-	-	-
Generator	2	59	118	Generator	2	20	40
Rectifier	2	29	58	-	-	-	-
Inverter	1	55	55	AC-AC Converter	2	13	26
Motor	1	109	109	Motor	2	20	40
Total			572	Total			106

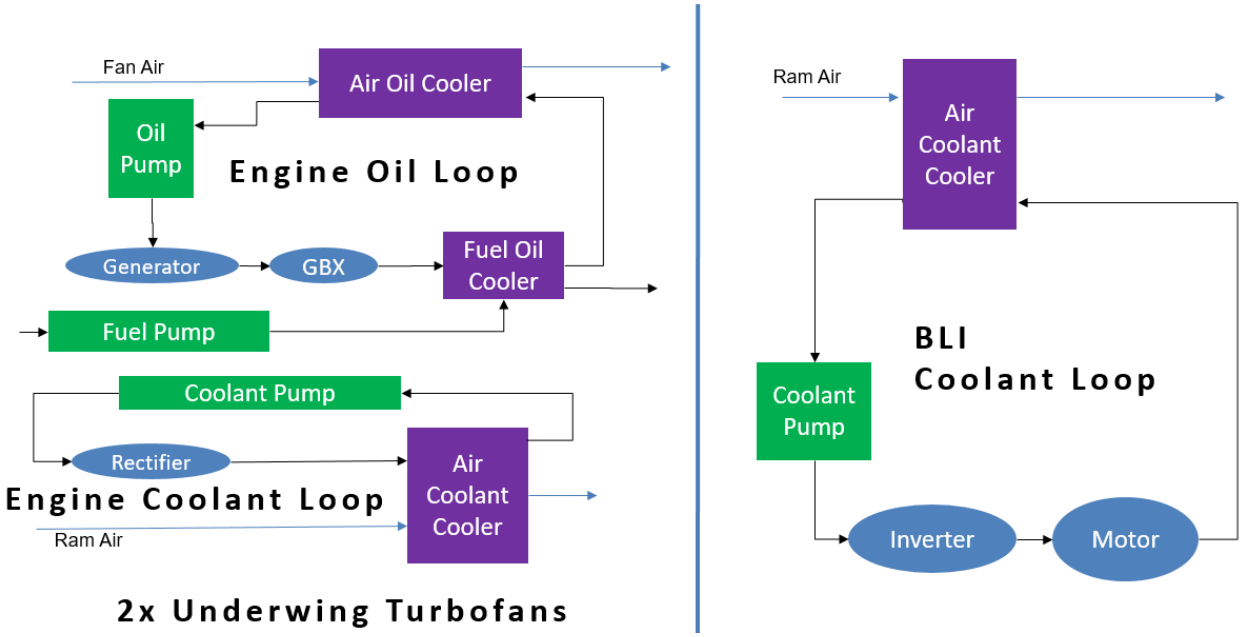

Figure 6. STARC-ABL baseline TMS architecture.

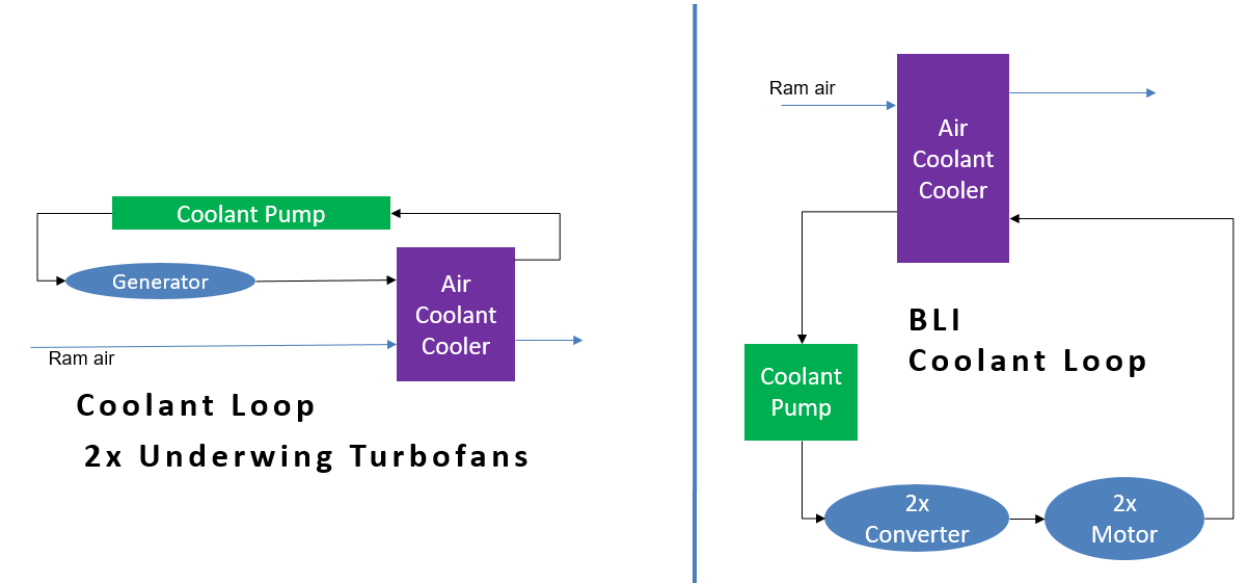

Figure 7. STARC-ABL advanced technology TMS architecture.

Based on the architectures, coolant choices and environmental parameters dictated by the RTO design point, three TMSs were created: baseline, corrected baseline, and advanced. For the design optimizations, an overall vehicle level STARC-ABL objective was generated through a sensitivity study that relates drag (lbf), power required by TMS (kW), and weight (kg) to % increase in fuel burn, as shown in equation 2.

$$FuelBurn_{\%increase} = (4.1 * Weight + 44.4 * Power + 1.5 * Drag) * 1e - 3 \quad (2)$$

The resulting weight, power required, and drag penalty for each design is shown in Table 6. The weights for the baseline, corrected baseline, and advanced configurations are 198 kg, 109 kg, and 51 kg, respectively. The differences in weight between the baseline and corrected baseline are exclusively from the engine oil loop correction. Assuming a linear reduction in loop weight as less heat is rejected, the 54 kg engine oil loop is estimated to be reduced by 70%, which corresponds to an estimated 16 kg corrected baseline; however the optimization results in a 10.08 kg mass. This difference is due to the FOC, which actually gains size with less energy in the system, because the oil mass flow required to maintain component temperature limits is reduced. In both the engine coolant loop and the BLI loop, the rejected power is lower in the advanced configuration; however, the temperature limits are also decreased and the coolant fluid was updated from PGW30 to PSF-5 (coolant specific heat is reduced). Although the temperature requirements are more stringent for the advanced concept, the weight is reduced by more than half. The TMS required power is significantly less than 1 kW for each of the designs. However, the required power of the advanced concept is larger due to the higher viscosity of PSF-5, compared with that of PGW30. Comparing drag for the three configurations, it can be seen that the baseline and corrected baseline are similar in magnitude and the advanced configuration is roughly 35% of the corrected baseline. The small difference between the corrected baseline and baseline drag values highlight the relatively low drag penalty of utilizing engine bypass air, where high pressure gains can be leveraged to minimize mass flow rates and overall loss of thrust.

Table 6. STARC-ABL TMS design metrics.

TMS Loop		**Baseline (includes gearbox cooling)**	**Corrected Baseline (includes only electric system cooling)**	**Advanced**
Engine oil loop (2x)	Weight (kg)	54.40	10.08	None
	Power required (kW)	0.04	0.01	None
	Drag (lbf)	2.25	1.46	None
Engine Coolant loop (2x)	Weight (kg)	15.30	15.30	9.46
	Power required (kW)	0.03	0.03	0.05
	Drag (lbf)	1.83	1.83	0.74
BLI loop	Weight (kg)	58.57	58.57	31.85
	Power required (kW)	0.06	0.06	0.21
	Drag (lbf)	6.53	6.53	3.05
Total:	Weight (kg)	197.97	109.33	50.77
	Power required (kW)	0.20	0.14	0.31
	Drag (lbf)	14.68	13.11	4.52

D. RVLT Tiltwing

The EAP system for the RLVT tiltwing consists of a single turboshaft engine electrically driving four wing-mounted propellers, as shown in Figure 8. In the baseline electrical system, the turboshaft runs a generator to produce power that is converted to DC for the DC bus. Power is then converted again for each of the four motors powering the propellers. In the advanced electrical system, turboshaft power is run directly to the AC bus then delivered to each motor via an AC to AC conversion utilizing a DC-link converter. The heat load from the electrical system is summarized in Table 7. Here it can be seen that utilizing the advanced technology offers a roughly 3 times reduction in losses (not including the engine gearbox). Since the tiltwing utilizes roughly 3 times more power at hover than it does at cruise, hover will be used as the sizing point for the following designs.

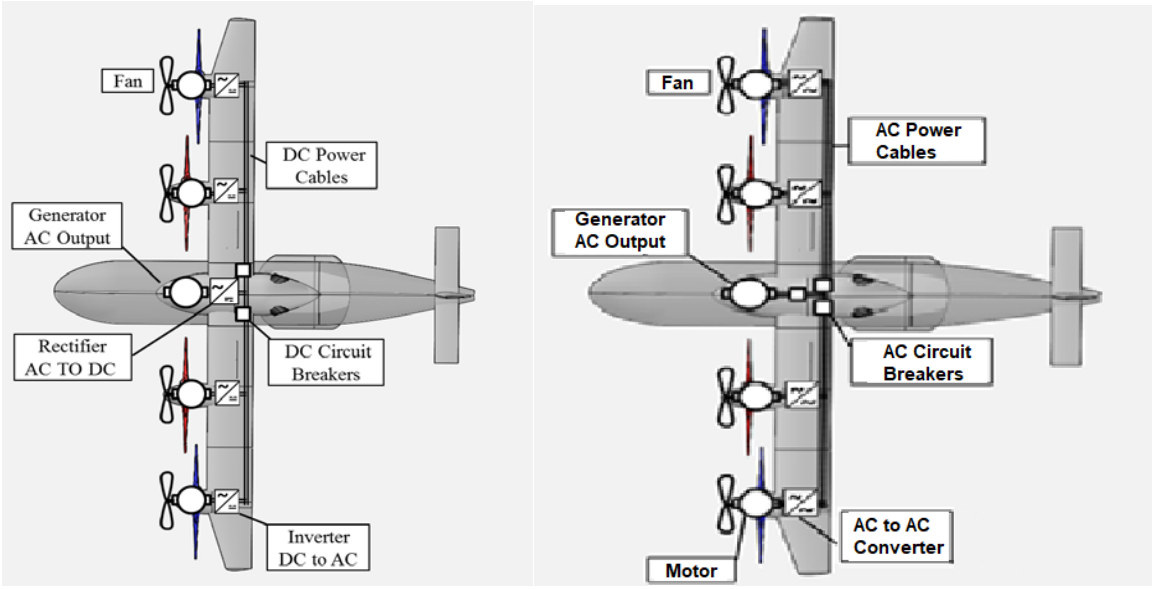

Figure 8. RVLT EAP architecture for baseline (left) and advanced concepts (right).

Table 7. RVLT tiltwing heat losses.

Baseline				Advanced			
Component	**Qty**	**Loss (kW)**	**Total loss (kW)**	**Component**	**Qty**	**Loss (kW)**	**Total loss (kW)**
Gearbox	1	72	72	-	-	-	-
Generator	1	101	101	Generator	1	35	35
Rectifier	1	48	48	-	-	-	-
Inverter	4	12	48	AC-AC Converter	4	6	24
Motor	4	23	92	Motor	4	8	32
Total			361	Total			91

The baseline TMS architecture for the RVLT tiltwing is shown in Figure 9. In this design, two main types of cooling loops are developed. The first type, which uses PGW30 as a coolant, gathers heat from the loads and rejects them using an air-to-coolant heat exchanger. Due to the static nature of the hover condition, puller fans are utilized to increase the pressure ratio across each heat exchanger. The motors are also cooled in series with the power electronics to reduce complexity. The second type of cooling loop utilizes oil as the coolant. Similar to the STARC-ABL an engine cooling loop will exist to cool the engine gearbox, accessories, and bearings. Oil has a much higher operating temperature than PGW30, so the baseline technology generator, which can also operate at a high temperature, is placed on the engine cooling loop. In this case it was decided to not include a FOC because of the incurred weight penalty and the reduced mission length.

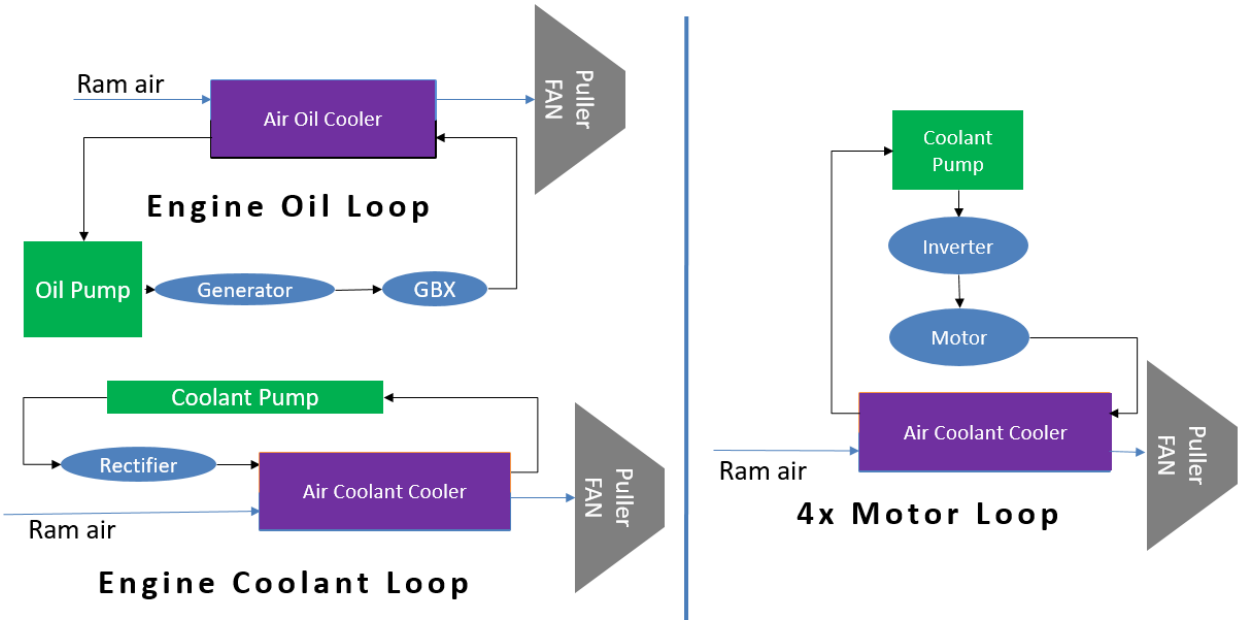

Figure 9. RVLT tiltwing baseline TMS architecture.

The advanced TMS architecture for the RVLT tiltwing is shown in Figure 10. Here each loop utilizes the PSF-5 cooling fluid. Architectures for the power electronics and motors are identical to those found within the baseline version. Cooling for the advanced technology generator has been removed from the oil loop due to the reduced temperature limits associated with the HEMM, and placed on a separate cooling loop.

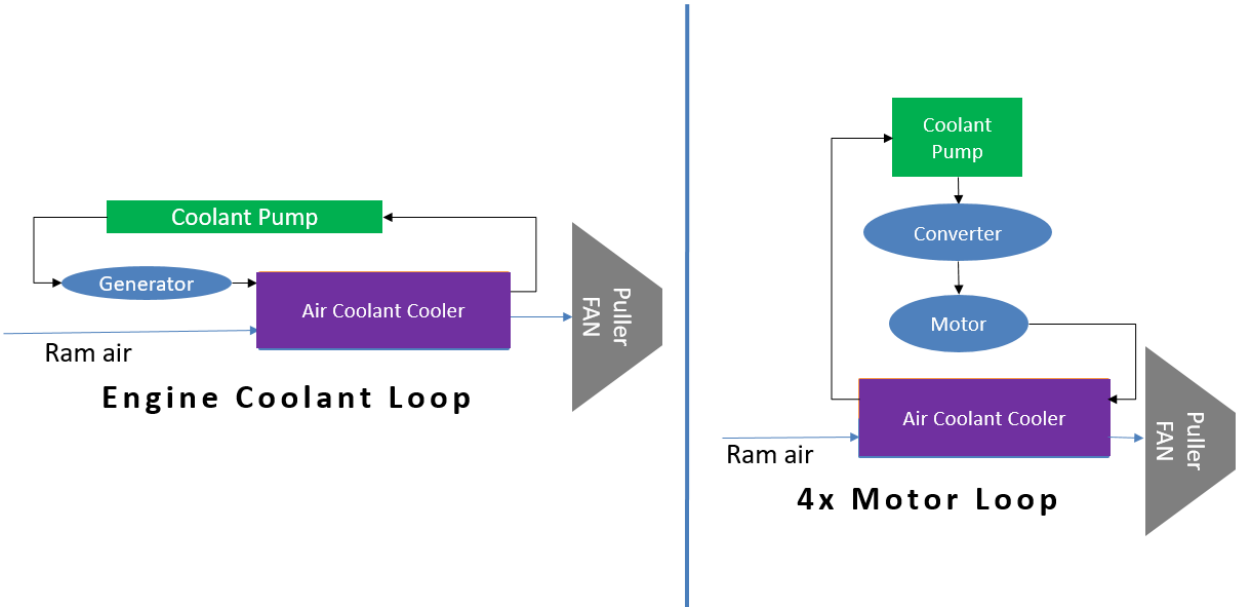

Figure 10. RVLT tiltwing advanced technology TMS architecture.

Design optimizations for the tiltwing TMS architecture were run using an objective tuned for a hover design point as shown in equation 3 as a function of weight (kg), power (kW), and drag (lbf). Comparing the tiltwing objective

with the STARC-ABL objective, it can be seen that the objective weight for required power and thrust are lower than those in the STARC-ABL. Results from the optimization are shown in Table 8. Here it can be seen that the use of puller fans causes the required power levels to be in the kW range for each of the baseline loops and net thrust is being generated (negative drag). When comparing the corrected baseline with the advanced designs, it is seen that the overall system weight is reduced by roughly 50%. The required power and net thrust are reduced by 60% as mass flow requirements are reduced due to lower heat loads. The motor loop weight decreases by 35% while the engine coolant loop by 20%, however the engine loop cools the rectifier in the baseline and in the advanced configuration it is cooling the generator and the engine oil loop is removed entirely. This shows the largest reduction in TMS size is a result from the move to the AC bus, which enables the removal of the engine side rectifier cooling loop (11.05 kg). In addition, in comparing the advanced generator cooling loop with that of the corrected baseline, it is noticed that weight actually increases from 7.21 kg to 8.62 kg due to the lower temperature cooling requirements.

$$FuelBurn_{\%increase} = 6.6e-2.0 * Weight + 2.0e-4.0 * Power + 1.1e-0.9 * Drag \quad (3)$$

Table 8. Tiltwing TMS design metrics.

Tiltwing	Metric	Baseline	Corrected baseline	Advanced
Motor loop (4x)	Weight (kg)	7.11	7.11	4.58
	Power required (kW)	1.36	1.36	0.60
	Drag (lbf)	-5.058	-5.058	-2.19
Engine oil loop*	Weight (kg)	14.55	7.21	-
	Power required (kW)	2.84	1.61	-
	Drag (lbf)	-11.13	-6.43	-
Engine coolant loop*	Weight (kg)	11.05	11.05	8.62
	Power required (kW)	2.26	2.26	1.41
	Drag (lbf)	-8.55	-8.55	-5.14
Total:	Weight (kg)	54.04	46.7	26.94
	Power required (kW)	10.54	9.31	3.81
	Drag (lbf)	-39.92	-35.21	-13.89

* Note: in the baseline configuration the generator is cooled within the engine oil loop and the rectifier is cooled within the engine coolant loop, however in the advanced configuration the generator is cooled within the engine coolant loop and the rectifier cooling loop has been removed.

E. PEGASUS

The EAP system for the PEGASUS consists of two wing-mounted propellers, a BLI propeller, and two wing tip mounted propellers, as shown in Figure 11. A centrally located battery is connected to each of the propulsors via a DC bus. Motors and their drivers then pull the required power from this bus. In this case the baseline and advanced EAP architectures are the same. This similarity occurs because the battery will be producing DC power directly, which, in contrast with the previous two concepts, the power is taken from a gas turbine driven generator that produces AC power. As this paper only considers the all-electric mission, the wing mounted engines have been neglected in the design.

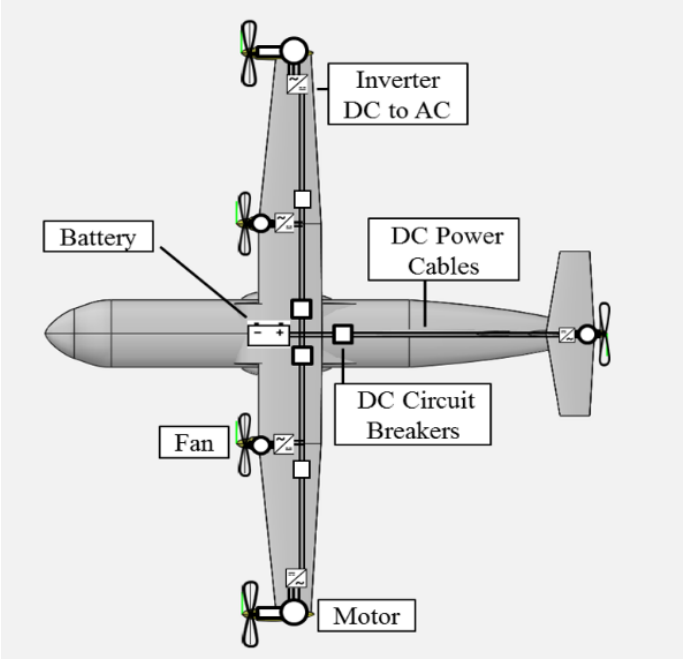

Figure 11. PEGASUS EAP architecture for baseline and advanced concepts.

The PEGASUS heat loads and a diagram of TMS architecture are located in Table 9 and Figure 12, respectively. The listed loads are for potential RTO and Cruise design points. During RTO, inboard motors provide the majority of the thrust. On the other hand, these inboard motors shut down during cruise while the tip motors increase their load. During both mission segments, the BLI motors use a constant amount of power. The inverter and motor losses for the advanced technology are 77% and 65% lower than the baseline, respectively. Battery power losses, on the other hand, remain fairly consistent between the two technology levels due to a constant efficiency assumption. The TMS architecture is modularized with loops consisting an inverter and motor for the tip, inboard, and BLI components with the battery split off on the second loop type. The overall power reduction for each combined loop (motor and inverter) is roughly 70%. In the baseline configuration, all loops utilize PGW30, but in the advanced configuration, the tip, inboard, and BLI loops utilize PSF-5 coolant. The battery cooling loops in the advanced and baseline both use PGW30 coolant.

Table 9. PEGASUS heat losses for baseline and advanced configurations.

		Baseline		Advanced		
Component	**Qty**	**Loss (kW)**	**Total loss (kW)**	**Loss (kW)**	**Total loss (kW)**	**Design Point**
Tip Inverter	2	9	18	2	4	RTO
Tip Motor	2	15	30	4	8	RTO
Tip Inverter	2	17	34	4	8	Cruise
Tip Motor	2	33	66	12	24	Cruise
Inboard Inverter	2	22	44	5	10	RTO
Inboard Motor	2	44	88	16	32	RTO
Inboard Inverter	2	0	0	0	0	Cruise
Inboard Motor	2	0	0	0	0	Cruise
BLI Inverter	1	11	11	3	3	All
BLI Motor	1	22	22	8	8	All
Battery	1	297	297	285	285	RTO
Battery	1	186	186	178	178	Cruise
Total			542		381	RTO
Total			301		229	Cruise

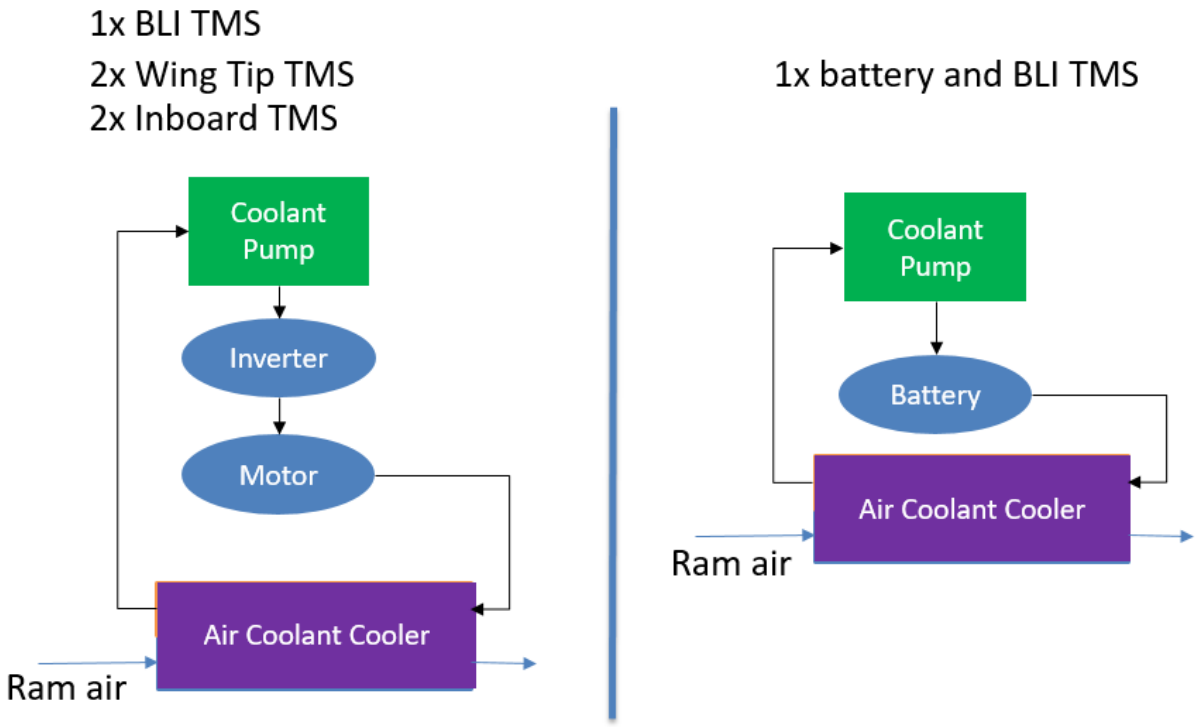

Figure 12. PEGASUS TMS architecture for baseline and advanced TMS architectures.

Utilizing the architecture in Figure 12, simulations were run for each loop at the Cruise and RTO design points. An optimization objective was calculated based on the PEGASUS sensitivity of electrical energy used related to the three TMS metrics, weight (kg), power required (kW), and drag (lbf), as shown in equation 4. Final design points for each loop were chosen on a case-by-case basis between the loads at RTO and cruise. For the tip, inboard, and BLI loops, RTO was found to be the limiting case despite the tip motors and electronics running at twice the power at cruise. Alternatively, it was found that cruise is the limiting case for the battery. This is because at cruise, the battery must use the constant power temperature limit (35 C), but for takeoff a limited time temperature limit can be used, which is higher than the constant power limit (54 C).

$$EnergyUsed_{kJ\ used} = 3.5e2 * Weight + 6.5 * Power + 2.0e2 * Drag \quad (4)$$

The completed designs for the two technology levels is shown in Table 10, which shows the baseline and advanced configurations weight as 196 kg and 139 kg, respectively (30% weight reduction). The battery metrics are similar between the two technology levels, because constant efficiency was assumed. A weight comparison between the baseline and advanced configuration, without considering the battery TMS, results in a weight saving of 55%. Similarly, in comparing overall TMS required power and drag, excluding the battery, results in a 200% increase and 50% reduction respectively. This increase in TMS required power is due to the rise in viscosity associated with the coolant used in the advanced configuration, but all power levels were significantly less than 1 kW. The reduction in drag corresponds to the lower power rejection requirements for the advanced configuration.

Table 10. PEGASUS TMS design metrics.

		Baseline	**Advanced**
Battery loop	Weight (kg)	100.19	96.01
	Power required (kW)	0.16	0.15
	Drag (lbf)	10.58	10.17
Inboard loop (2x)	Weight (kg)	28.20	12.90
	Power required (kW)	0.02	0.05
	Drag (lbf)	2.16	0.81
Tip loop (2x)	Weight (kg)	11.98	4.78
	Power required (kW)	0.01	0.01
	Drag (lbf)	0.83	0.23
BLI loop	Weight, (kg)	15.00	7.52
	Power required (kW)	0.01	0.03
	Drag (lbf)	1.08	0.43
Total:	Weight (kg)	195.55	138.89
	Power required (kW)	0.22	0.30
	Drag (lbf)	17.64	12.67

IV. Cross Vehicle Comparison

In this paper three full TMS systems have been developed with their respective design constraints and environmental conditions. Although these systems were developed independently, several TMS cooling loop architectures reoccur across each vehicle type. The most prominent of these is the power converter, motor cooling loop (converter + motor), developed at the RTO (or Hover for the tiltwing) design point. To study the differences in the designs, each cooling loop developed for the three vehicles has been plotted against its respective heat load rejected. These cooling loops demonstrate how the designs change with heat load rejection and objective function. Additionally, power sweeps in TMS design are shown for the converter + motor cooling loops of each vehicle and technology level. These sweeps demonstrate the potential designs and allow for the comparison of design applications. For example, a design for battery cooling could be compared to a design for the converter + motor for the same heat

load rejected. A comparison of all converter + motor trends is displayed in figures 13 through 15, where the baseline trends are represented by solid lines while the advanced counterparts are represented by dashed curves. To show how these specific trends compare with other cooling loops in the vehicle (e.g. The STARC-ABL Engine + generator loop), individual markers corresponding to these loops are placed and color-coded to their associated vehicle. The data used in the following section is located within the appendix.

From the TMS design weights, as shown in Figure 13, it can be observed that the individual "loop-level" results are lower for the baseline cases, at a given power, than the advanced cases. However, when changes in heat load are account for, the advanced TMS designs turn out smaller since their heat load is smaller. Figure 13 also shows that the different objectives used for the three vehicles have a profound effect on the weight of the vehicle TMS designs. Weights for the tiltwing are generally lower than those of the PEGASUS or STARC-ABL, because the tiltwing is more sensitive to weight due to the requirement for hover. Architecture loops for cooling the battery and the engine + generator offer the largest deviations from the converter + motor loop architecture. Although the battery utilizes a cooling loop architecture similar to the converters, its design weight is higher due to stricter temperature limitations on the component. Conversely, the engine + generator loops show significantly lower weight than similarly designed cooling loops due to the higher cooling fluid temperatures and efficiencies in combining the engine cooling loop with the engine hardware.

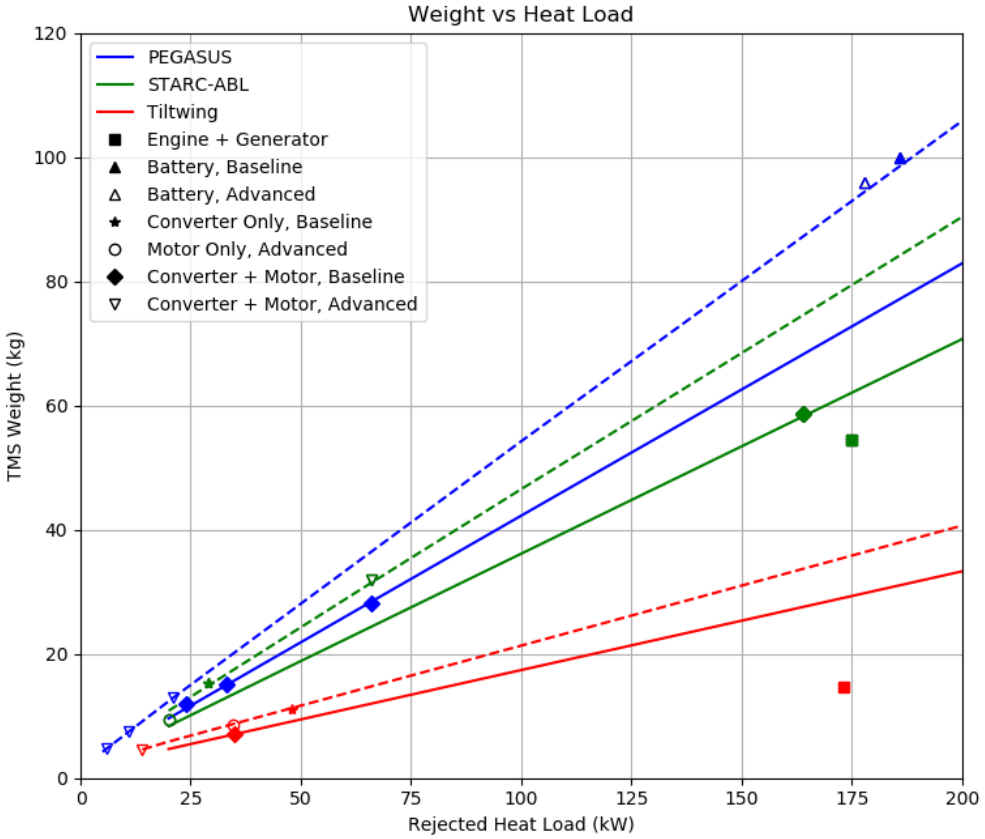

Figure 13. TMS loop weight values and rejected power sensitivity comparison, where markers and lines that are blue show PEGASUS, green show STARC-ABL, and red tiltwing. Additionally, solid lines denote baseline and dotted lines denote advanced electrical system technology levels.

Required power comparison traces are, shown in Figure 14 with a logarithmic scale (Note: curves revealed to be lines with a typical scale). In these trends it can be seen that the baseline configurations have much lower required power than the advanced configurations due to their coolant properties being more favorable than those of PSF-5. The tiltwing required power is also much higher due to the high relative objective weighting to weight. Similar to weight, battery and engine + generator required powers are higher and lower than the converter + motor designs, respectively.

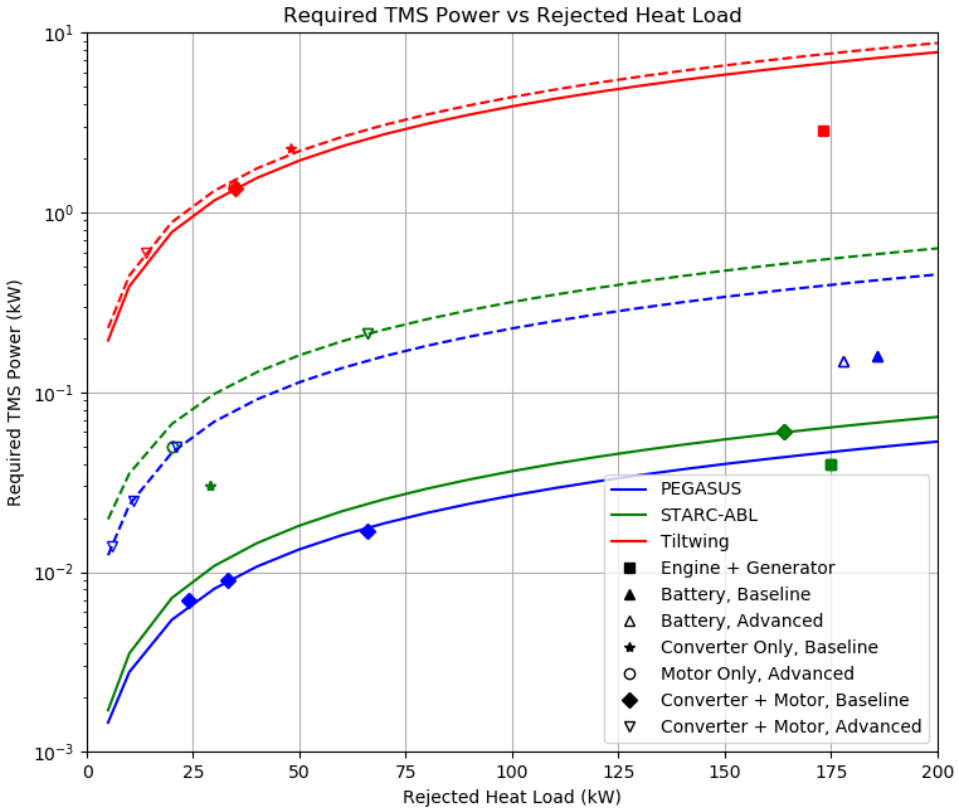

Figure 14. TMS loop required power values and rejected power sensitivity comparison, where markers and lines that are blue show PEGASUS, green show STARC-ABL, and red tiltwing. Additionally, solid lines denote baseline and dotted lines denote advanced electrical system technology levels.

A drag comparison is shown in Figure 15, where it can be seen that drag values for the PEGASUS and STARC-ABL (including baseline and advanced technologies) are within 5 lbf of the converter + motor loops throughout every design. The converter + motor configuration for the tiltwing is negative due to thrust being produced through the use of puller fans. The thrust values for the battery are slightly higher than the predicted converter + motor cooling loops and the thrust values for the engine + generator are lower. With the tiltwing this lower thrust is generated by the cooling system and for the STARC-ABL and PEGASUS this is less drag. Both of these reductions are due to a reduced mass flow requirement that comes from a more efficient cooling system.

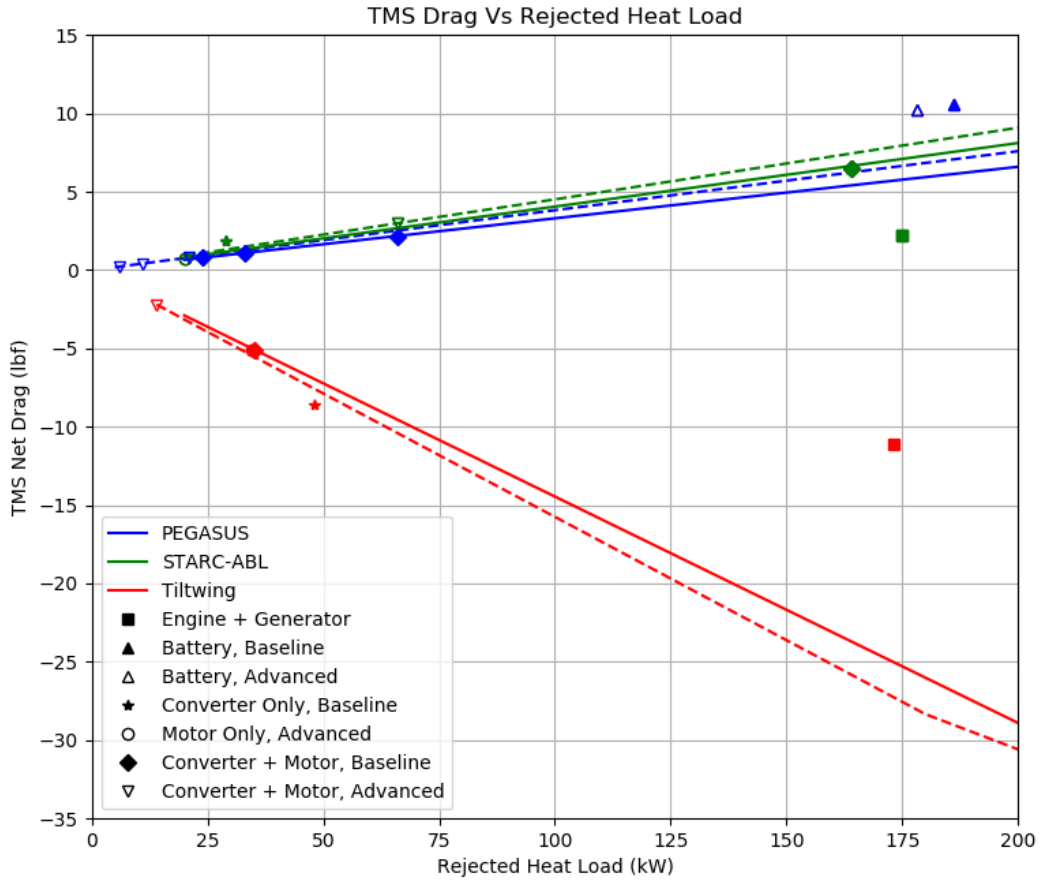

Figure 15. TMS loop drag values and rejected power sensitivity comparison, where markers and lines that are blue show PEGASUS, green show STARC-ABL, and red tiltwing. Additionally, solid lines denote baseline and dotted lines denote advanced electrical system technology levels.

As one can see from figures 13 to 15, the results for the different loops trend well with the converter+motor loop trends for the same vehicle. While the differences are more significant for the tiltwing, it appears that the mass contribution of these other TMS elements can be approximated to a fair degree by the converter-motor trend. As such, simple sizing relations can be developed to facilitate a simple preliminary system design, as shown in Table 11 (based on the converter + motor cooling loops). For certain unrepresented cooling loops where temperature limits are much different, such as the PEGASUS battery cooling loop or the STARC-ABL baseline engine + generator loop, error will result from using these relations. In addition, environmental design factors (such as altitude and MN) will shift these sizing relations. For these reasons, a full analysis should be done as more complexity can be added to the system model to facilitate a better estimate of loop metrics and proper design points. It should also be noted that these are design values only, and drag and required power may change significantly during off-design operation due to changes in environmental conditions or TMS loading.

Table 11. On design (RTO) sizing relations for loops cooling converters in series with motors.

Vehicle Objective	Technology Level	Coolant	TMS Sizing Relations, weight(kg), power(kW), and drag (lbf)
STARC-ABL	Baseline	PGW30	$\text{weight} = 0.346 * power_{rejected} + 1.480$ $power_{required} = 3.65\text{e}-4 * power_{rejected} - 1.19\text{e}-4$ $\text{drag} = 4.06\text{e}-2 * power_{rejected} + 4.41\text{e}-5$
STARC-ABL	Advanced	PSF-5	$\text{weight} = 0.442 * power_{rejected} + 2.195$ $power_{required} = 3.13\text{e}-3 * power_{rejected} + 4.01\text{e}-3$ $\text{drag} = 4.55\text{e}-2 * power_{rejected} - 1.05\text{e}-2$
RVLT Tiltwing	Baseline	PGW30	$\text{weight} = 0.159 * power_{rejected} + 1.4824$ $power_{required} = 3.88\text{e}-2 * power_{rejected} + 8\text{e}-8$ $\text{drag} = -0.1446 * power_{rejected} + 0.0025$
RVLT Tiltwing	Advanced	PSF-5	$\text{weight} = 0.1902 * power_{rejected} + 1.8401$ $power_{required} = 4.36\text{e}-2 * power_{rejected} + 9.2\text{e}-3$ $\text{drag} = -0.1532 * power_{rejected} - 0.0228$
PEGASUS	Baseline	PGW30	$\text{weight} = 0.407 * power_{rejected} + 1.504$ $power_{required} = 2.65\text{e}-4 * power_{rejected} + 1.33\text{e}-4$ $\text{drag} = 3.30\text{e}-2 * power_{rejected} + 5.87\text{e}-3$
PEGASUS	Advanced	PSF-5	$\text{weight} = 0.5207 * power_{rejected} + 1.863$ $power_{required} = 2.25\text{e}-3 * power_{rejected} + 1.15\text{e}-3$ $\text{drag} = 3.80\text{e}-2 * power_{rejected} + 1.11\text{e}-2$

V. Summary and Conclusions

This paper details the TMS design for three electrified aircraft propulsion (EAP) concepts at two distinct electrical system technology levels (state-of-the-art or baseline and advanced). These TMS designs utilize compact plate-fin type heat exchangers within a conventional fluid-based TMS architecture. Results show that, while the advanced technology level TMS designs result in higher weight per rejected power, the overall weight of the advanced technology concepts were lower due to increased efficiencies. Specifically, it is found that utilizing advanced electrical systems can reduce TMS weight, power used, and drag, and that the roughly 1.5% increase in electrical converter efficiency, 2.5% increase in motor efficiency, along with utilizing an AC bus to allow for the removal of a rectifier, resulted in a roughly 50% reduction in TMS weight for the considered systems. The EAP systems considered within this paper are NASA concepts: the STARC-ABL single aisle aircraft, a turbo-electric tiltwing VTOL vehicle, and the PEGASUS regional aircraft. Results from the vehicle studies show that, given a constant rejected heat load, design weights for CTOL vehicles (STARC-ABL and PEGASUS) are higher than the VTOL vehicle (tiltwing). This is because the tiltwing is shown to be much more sensitive to TMS weight than power used, which is compounded because TMS power is generated from relatively light weight fuel, rather than a heavy battery. A sizing study in this paper shows that TMS weight, power usage, and drag generally increase linearly with increases in required rejected heat load given constant flow temperatures. An additional sizing study was performed to show TMS designs developed at different points along a notional mission profile. This study demonstrates that designing the TMS at rolling takeoff will result in the heaviest systems assuming constant heat load. Cooling loops for each vehicle are analyzed separately and sizing relations are developed for a generalized power converter and motor cooling loop. These sizing relations demonstrate a rough estimate of the TMS size, power required, and drag penalty before performing a full TMS design.

Appendix

Table 12. Cooling loop comparison.

Loop Type	Platform	Technology	Rejected Power, kW	Coolant	Weight, kg	Required power, kW	Drag, lbf
engine + generator	STARC-ABL engine	baseline	175	engine oil	5.44E+01	4.00E-02	2.25E+00
	Tiltwing	baseline	173	engine oil	1.46E+01	2.84E+00	-1.11E+01
converter	STARC-ABL engine	baseline	29	PGW30	1.53E+01	3.00E-02	1.83E+00
	Tiltwing	baseline	48	PGW30	1.11E+01	2.26E+00	-8.55E+00
battery	PEGASUS battery	baseline	186	PGW30	1.00E+02	1.60E-01	1.06E+01
		advanced	178	PGW30	9.60E+01	1.50E-01	1.02E+01
converter + motor	STARC-ABL BLI	baseline	164	PGW30	5.86E+01	6.00E-02	6.53E+00
	PEGASUS inboard	baseline	66	PGW30	2.82E+01	1.70E-02	2.16E+00
	PEGASUS tip	baseline	24	PGW30	1.20E+01	7.00E-03	8.33E-01
	PEGASUS BLI	baseline	33	PGW30	1.50E+01	9.00E-03	1.08E+00
	Tiltwing	baseline	35	PGW30	7.11E+00	1.36E+00	-5.06E+00
motor (HEMM)	STARC-ABL engine	advanced	20	PSF-5	9.46E+00	5.00E-02	7.36E-01
	Tiltwing	advanced	34.6	PSF-5	8.62E+00	1.41E+00	-5.14E+00
converter + motor (HEMM)	STARC-ABL BLI	advanced	66	PSF-5	3.19E+01	2.12E-01	3.05E+00
	PEGASUS inboard	advanced	21	PSF-5	1.29E+01	5.00E-02	8.10E-01
	PEGASUS tip	advanced	6	PSF-5	4.78E+00	1.40E-02	2.25E-01
	PEGASUS BLI	advanced	11	PSF-5	7.52E+00	2.50E-02	4.28E-01
	Tiltwing	advanced	14	PSF-5	4.58E+00	6.00E-01	-2.19E+00

References

[1] Jansen, J. H., Bowman, C., Jankovsky, A., Dyson, R., Felder, J., "Overview of NASA Electrified Aircraft Propulsion Research for Large Subsonic Transports," AIAA Propulsion and Energy Forum, Atlanta, GA. 2017.

[2] Shahab, H., "Urban Air Mobility (UAM) Market Study," HQ-E-DAA-TN70296, 2019.

[3] Goyal, R., "Urban Air Mobility (UAM) Market Study," NASA/HQ-E-DAA-TN65181, 2018.

[4] Welstead, J. R., Felder, J. L., "Conceptual Design of a Single-Aisle Turboelectric Commercial Transport with Fuselage Boundary Layer Ingestion," AIAA SciTech Forum, San Diego, CA. 2016.

[5] Johnson, W., Silva, C., Solis, E., "Concept Vehicles for VTOL Air Taxi Operations," AHS Technical Conference on Aeromechanics Design for Transformative Vertical Flight, San Francisco, CA, Jan. 16-19, 2018.

[6] Antcliff, K., Capristan, F., "Conceptual Design of the Parallel Electric-Gas Architecture with Synergistic Utilization Scheme (PEGASUS) Concept," 18th AIAA/ISSMO Multidisciplinary Analysis and Optimization Conference, AIAA 2017-4001, Denver, CO, June 5-9, 2017.

[7] Capristan, F., Blaesser, N., "Analysis of the Parallel Electric-Gas Architecture with Synergistic Utilization Scheme (PEGASUS) Concept," NASA/TM–2019–220396, Aug, 2019.

[8] O'Connell, T., Haran, K., Lents, C., Bayles, B., "Enabling Technologies & Analysis Methods for More-, Hybrid-, and All-Electric Aircraft," AIAA Propulsion & Energy Forum Short Course, Cincinnati, OH, July 8-11, 2018.

[9] Chapman, J., Schnulo, S., Nitzche, M., "Development of a Thermal Management System for Electrified Aircraft," AIAA Science and Technology Forum, AIAA 2020-0545, Orlando, FL, Jan. 6-10, 2020.

[10] Jansen, R., Avanesian, D., Schnulo, S., Antcliff, K., "HEATheR: High-Efficiency Aircraft Thermal Research," EnergyTech2019 Conference and Exposition, Cleveland, Oh, Oct. 21-25, 2019.

[11] Jansen, R., Kascak, P., Dyson, R., Woodworth, A., Scheidler, J., Smith, A., Stalcup, E., Tallerico, T., De Jesus-Arce, Y., Avanesian, D., "High Efficiency Megawatt Motor Preliminary Design," AIAA/IEEE Electric Aircraft Technologies Symposium, AIAA 2019-4513, Indianapolis, IN, August 22-24, 2019.

[12] Sadey, D., Csank, J., Hanlon, P., Jansen, R., "A Generalized Power System Architecture Sizing and Analysis Framework," AIAA Propulsion and Energy Forum, AIAA 2018-4616, Cincinnati, OH, July 9-11, 2018.

[13] Azurza, J., Hanak, E., Schrittwieser, L., Johann, K., Deboy, G., "Towards a 99.5% Efficient All-Silicone Three-Phase Seven-Level Hybrid Active Neutral Point Clamped Inverter," 2018 IEEE International Power Electronics and Application Conference and Exposition (PEAC), 2018.8590488, November, 2018.

[14] Lithium-ion rechargeable cell for power tools, Spec No. INR18650-25R, Rev. 1, Samsung SDI, Mar. 2014.

[15] Schnulo, S., Chapman, J., Hanlon, P., Sadey, D., Sozer, E., Bhamidapati, K., Kirk, J., "Assessment of the Impact of an Optimal Power System on a Turboelectric Single Aisle Concept Aircraft," to be presented at the AIAA/IEEE Electric Aircraft Technologies Symposium (EATS), August 26-28, 2020.

[16] Kays, W.M., London, A.L., *Compact Heat Exchangers*, 3rd Ed., Krieger Publishing Co., Malabar, Florida, 1984.

[17] Gray, J., Hwang, J., Martins, J., Moore, K., Naylor, B., "OpenMDAO: An Open-Source Framework for Multidisciplinary Design, Analysis, and Optimization," Structural and Multidisciplinary Optimization, 2019.

[18] Gill, P., Murray, W., Saunders, M., Wong, E., "SNOPT 7.7 User's Manual," CCoM Technical Report 18-1, Center for Computational Mathematics, University of California, San Diego.

[19] Rheaume, J. M., Macdonald, M., Lents, C.E., "Commercial Hybrid Electric Aircraft Thermal Management System Design, Simulation, and Operation Improvements," AIAA Propulsion and Energy Forum, AIAA 2019-4492, Indianapolis, IN, August 19-22, 2019.